INFLUENCE OF VANADIUM NANOCLUSTERS IN HYDROGEN UPTAKE USING HYBRID NANOSTRUCTURED MATERIALS

Juliana M. Juárez*, Jorgelina Cussa, Marcos B. Gómez Costa, Oscar A. Anunzaita

[a] *Centro de Investigación en Nanociencia y Nanotecnología (NANOTEC), Facultad Regional Córdoba, Universidad Tecnológica Nacional, Maestro López y Cruz Roja Argentina, 5016, Córdoba, Argentina*

**E-mail: jjuarez@frc.utn.edu.ar*

Resumen

En el presente trabajo se presenta la síntesis y caracterización de nanoclusters de oxidos de vanadio (V_2O_5) soportados en un material nanoestructurado de silicio (SBA-15) y en un material nanoestructurado de carbono (CMK-3). Este material presenta características prometedoras para ser utilizado en la adsorción de hidrógeno.

Los distintos materiales modificados con nanoclusters de oxidos de vanadio (V_xO_y-SBA-15 and V_xO_y-CMK-3) se lograron sintetizar exitosamente y fueron caracterizados mediante Difracción de Rayos X, Propiedades Texturales, XPS y TEM. VxOy-SBA-15 and VxOy-CMK-3 mejoraron notablemente la adsorción de hidrogeno (1.33 %p/p y 3.43 %p/p a 77 K y 10 bar) comparados con sus soportes SBA-15 y CMK-3 respectivamente. Estos materiales son prometedores para la adsorción de hidrógeno mediante débiles fuerzas de interacción (fisisorción).

Palabras clave: Carbon mesoporoso, V-CMK-3, Hidrogeno, Adsorción.

Abstract

In this work, the synthesis and characterization of vanadium oxide nanoclusters (V_2O_5) supported in silica nanostructured material (SBA-15) and nanostructured carbon (CMK-3) is presented. This material is promising in hydrogen adsorption and storage application for energy harvesting.

The materials with vanadium oxide nanoclusters (V_xO_y-SBA-15 and V_xO_y-CMK-3) were successfully synthesized and characterized by X-ray diffraction, Textural properties, UV–Vis–DRS, X-Ray Photoelectron Spectroscopy and Transmission Electron Microscopy analyses. V_xO_y-SBA-15 and V_xO_y-CMK-3 improved significantly the H2 storage behavior (1.33 wt.% and 3.43 wt.% at 77K and 10 bar) compared with their respective supports SBA-15 and CMK-3. The materials synthesized are promising in hydrogen uptake by weak links forces (physisorption). A mechanism of hydrogen adsorption was proposed and V^{+5} cation roll in hydrogen uptake was discussed.

Keywords : Mesoporous carbon, V-CMK-3, hydrogen, adsorption.

1. Introducción

All over the world in the past decades, one of the most concerning subject is the fossil fuel reduction, along with the global warming issue. This both concerns have made hydrogen an ideal alternative to conventional fossil-fuel resources. Among the principal advantages of the use of hydrogen as an alternative is that it has the highest heating value per mass of all chemical fuels, is regenerative, it has a simple adsorption-desorption kinetics, environmentally friendly and it has low cost, [1]. Nevertheless, it has serious disadvantages, such as low volumetric and gravimetric densities, that limited its storage [2]. For that reason, several efforts have been made in order to develop an efficient, safe and cost effective method for hydrogen storage.

Several kind of materials have been matter of studies in this field, such as carbon nantubes, ordered mesoporous carbons (OMC), polymer nanocomposites, zeolites, Metal organic Frameworks (MOF) and other porous nanomaterials [3-5]. Nanoestructured carbons, like activated carbon fibers, carbon nanotubes and mesoporous carbons are suitable candidates for hydrogen adsorption due to their physical and chemical stability, high surface area and low cost among others [6-8].

One kind of ordered mesoporous carbons (OMC) are the carbon mesostructured from Korea (CMK). This kind of materials are synthesize by nanocasting strategy using mesoporous silicates as templates and have high surface area (from 1000 to 2000 m^2/g) and pore volumes in the range of 0.5 to 1 $ml.g^{-1}$. Accordingly, CMK-3 was chosen as a support material for hydrogen storage due to its large surface area, high chemical stability, uniform pore diameter, accessible porosity and three-dimensional conducting network [9-11].

On the other hand, among the siliceous mesoporous materials, SBA-15 presents regular networks and its pore diameter fluctuate thoroughly among 1.5 to 10 nm depending on the template. Because of their pore building and form, it is suitable as a probe material as an absorbent for a variety of gases and vapors [12, 13].

Some previous studies probed that H2 adsorption can be improved for mesoporous carbons introducing into the framework of the nanomaterial some metals or oxides, like platinum, Zn, ZnO, Ni, NiO, or TiO_2 [14-16]. Some other authors have made several efforts in the same direction, for instance, M. Konni et al. [17], incorporated iron and copper nanoparticles into multiwalled carbon nanotubes and studied their hydrogen adsorption.

In this work we studied the influence of the incorporation of vanadium nanoparticles inside the channels of two different supports such as the mesoporous silicate SBA-15 and into the mesoporous carbon CMK-3. This research includes the synthesis of the mesoporous silicate, and the synthesis of the CMK-3 by nanocasting strategy, the incorporation of the vanadium nanoclusters by wetness impregnation, the characterization of these nanomaterials by XRD, N_2 adsorption, XPS, TPR and Uv-Vis, TEM, and finally the study of the improvement in the hydrogen adsorption.

2. Experimental

Materials

Tetraethylorthosilicate (TEOS, 98%, Sigma–Aldrich), Poly(ethylene glycol)-block-poly(propylene glycol)-block-poly (ethylene glycol), ($EO_{20}PO_{70}EO_{20}$, P123-Sigma–Aldrich), Sucrose (≥99.0%, FLUKA) and Vanadium(III) chloride (99.999%, Sigma–Aldrich).

Synthesis of Si-SBA-15

The synthesis of the ordered mesoporous silica SBA-15 was prepared according to previous work [14].

Typically 20 g of P123 (Poly(ethylene glycol)-block-poly(propylene glycol)-block-poly (ethylene glycol)) was dissolved at 323 K in a HCl solution 1 M. Then, 40 g of TEOS was added and the resulting mixture was stirred at 323 K for 24 hours. The milky mixture was transferred into a Polypropylene bottle and it was kept at 373 K for 72 hours. The solid was filtered, washed with deionized water until pH ~6. The molar composition was Si: 0.018 $EO_{20}PO_{70}EO_{20}$: 2.08 HCl: 112 H_2O. To extract the template, the material was first immersed in ethanol reflux for 6 h. The product was filtered, washed, and dried in air at 363K, [18] To ensure the elimination of the structure-directing agent, it was heated under N_2 flow, at 20 / ml / min at 573K and then a calcined at 823 K in air for 6 h.

Synthesis of CMK-3 carbon

The synthesis of CMK-3 mesopourous carbon was carried out using SBA-15 as a hard template and sucrose as the carbon precursor following the synthesis procedure describe by Juárez et al. [14].

Briefly 1.1 g of sucrose was dissolved in a solution of H_2SO_4 (0.14 g) in water (5g), and to this solution it was added 1 g of SBA-15. The resulting mixture was dried at 373K and then was heated at

433 K for 6 hours. A second impregnation was performed in order to ensure the filling of the template pores with the carbon precursor, using an H_2SO_4 solution with 0.75 g of sucrose. The mixture was dried at 373 K and heated at 433K for 6 hours. Then this brown powder was heated to 1173K under nitrogen flow (20mL/min).

The silica removal was performed using a HF solution (5%wt) at room temperature. The carbon sample was filtered, washed with ethanol solution and dried at 393K.

Synthesis of VxOy-CMK-3 and VxOy -SBA-15

Vanadium nanoparticles were incorporated into ordered mesoporous carbon CMK-3 and into the siliceous mesoporous material SBA-15, using wetness impregnation and VCl_3 as source of Vanadium. The metal precursor (VCl_3) was dissolved in 20 mL of ethanol with vigorous stirring, to have a nominal content of 1 wt% of V in the final solid. The solution was placed in a rotary evaporator to remove excess of ethanol at about 323K and 50 rpm. The obtained powder was then dried at 373 K overnight in presence of air, in order to oxidize the vanadium species and avoid the carbon combustion. The resulting material was heated in a dynamic inert atmosphere (nitrogen flow of 20 mL/min) from 298 to 473K with a slope of 4 K/min and then the temperature was increased to 743K with a slope of 10 K/min and kept at this temperature during 5 h. The samples were denoted V_xO_y -SBA-15 and V_xO_y -CMK-3 respectively.

Characterization

The XRD patterns were recorded with a X'Pert Pro PANalytical diffractometer equipped with a CuKa radiation source (k = 0.15418 nm) and X'Celerator detector based on Real Time Multiple Strip (RTMS). The samples were ground and placed on a stainless steel plate. Diffractograms were analyzed with the X'PertHighScore Plus software. N_2 adsorption/desorption isotherms at 77 K were measured on ASAP 2020 equipment after degassing the samples at 673 K, determining textural properties such as surface area and pore volume; pore size distribution was estimated using the Barrett, Joyner and Halenda (BJH) algorithm. X-ray Photoelectron Spectra (XPS) were obtained on a MicrotechMultilb 3000 spectrometer, equipped with a hemispherical electron analyzer and MgKα (hν = 1253.6 eV) photon source. An estimated error of ±0.1 eV can be assumed for all measurements. Peak intensity was calculated from the respective peak areas after background subtraction and spectrum fitting by a combination of Gaussian/Lorentzian functions. Energy-dispersive X-ray analyses (EDX) were coupled to the scanning electron microscopy (SEM) LEO Mod. 440 equipment.

TEM were recorded in a JEOL 2100F microscope operated with an accelerating voltage of 200 kV (point resolution of 0.19 nm).

3. Resultados y discusión

X-ray diffraction

Low angle X-ray diffraction patterns for SBA-15, CMK-3, V^xO^y-SBA-15 and V^xO^y -CMK-3 are shown in Figure 1. The hard template SBA-15 shows excellent structural order for the hexagonal P6mm crystallographic space group. In the case of the mesopouros carbon CMK-3, obtained by hard templating of SBA-15, the pattern indicates that the carbon CMK-3 is an exact replica of the template, indicated by the appearance of peaks consistent with the symmetry of SBA-15, [19]. When the metal (vanadium) is incorporated to the structure the overall pore structure is maintained as indicated by the appearance of low-angle diffraction peaks. However, the intensity of the main peak [1 1 0] decrease compared to the pristine SBA-15 and CMK-3. This decrease might be due to the reduction of scattering contrast induced by the dispersed nanoparticles, [20]. Both vanadium modified samples reveals a shift to higher angle of 2Θ, indicating that the presence of vanadium species inside the framework of the support might increase the wall thickness, [21].

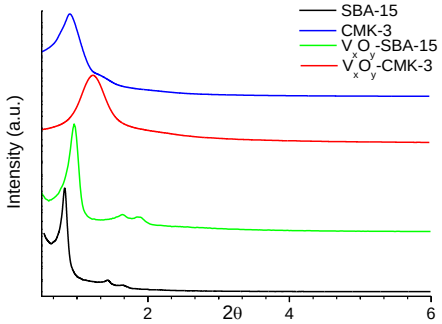

Figure 1. Small-angle XRD patterns of SBA-15, V_xO_y-SBA-15, CMK-3 and V_xO_y-CMK-3

Figure 2 shows the wide-angle X-ray diffraction patterns for CMK-3 and V_xO_y -CMK-3. In both cases two broad diffraction peaks are distinguished which can be indexed as [0 0 2] and [1 0 0] diffraction for typical graphite carbons, [22]. The wide-angle pattern of the samples SBA-15 and V_xO_y -SBA-15 are also shown in the Figure 2. It can be seen two broad peaks, characteristics for amorphous SBA-15 profiles [23]. In the wide-angle region practically no reflections typical of

vanadium have been found in any of the modified samples. The absence of this prominent reflection indicates that no crystalline bulk materials has been formed outside the pore system and it is an evidence that the clusters have nanometric size and high dispersion, [24]

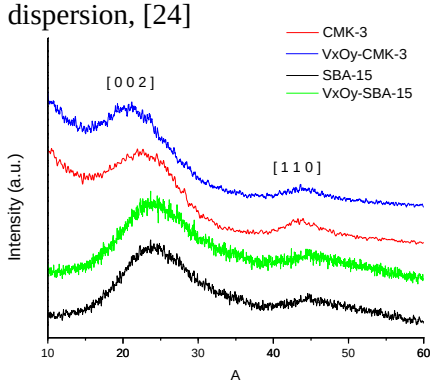

Figure 2. Wide-angle XRD patterns of SBA-15, V_xO_y-SBA-15, CMK-3 and V_xO_y-CMK-3

Textural properties - N2 adsorption-desorption isotherms

Figure 3 shows the N_2 adsorption/desorption isotherms of the different samples at 77 K, and Table 1 displays the textural properties determined from nitrogen physisorption analysis. For the siliceous samples SBA-15 and V_xO_y-SBA-15 we observe a type IV isotherm, with H1 type hysteresis loop, according with IUPAC classification, typical of ordered mesoporous materials.

The nitrogen adsorption–desorption isotherms for CMK-3 and VxOy -CMK-3 are typical type IV curves exhibiting hysteresis loops type H2, according to IUPAC classification, also typical of mesoporous solids. Materials obtained exhibit capillary condensation to relative pressures between 0.6 and 0.8 for the siliceous materials and between 0.40 and 0.45, which can be related to the pore blocking effect of affecting the pressure where evaporation/desorption pore occurs. The figure 3 also presents the pore size distributions of the different samples, showing sharp peaks that indicates a quite regular array of pores. The modified samples reveal a reduced specific surface area and pore diameter in comparison to those of pure SBA-15 and CMK-3 (Table 1) which implies the formation of nanoparticles of V_xO_y inside the mesoporous of the pristine SBA-15 and CMK-3.

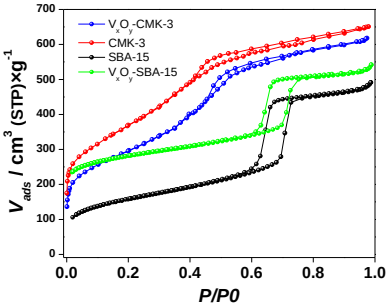

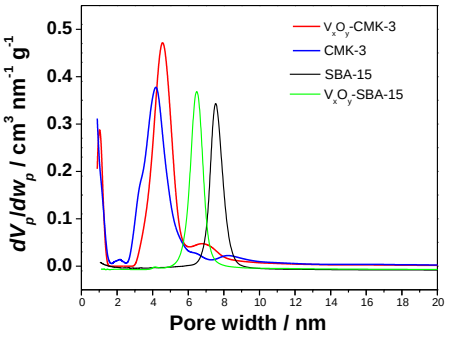

Figure 3. (a) N_2 adsorption/desorption isotherms of SBA-15, V_xO_y-SBA-15 and CMK-3 and V_xO_y-CMK-3 and (b) pore size distributions of SBA-15, V_xO_y-SBA-15 and CMK-3 and V_xO_y-CMK-3.

Table 1. Textural Properties

Material	S_{BET} (m^2 g^{-1})	V_{TP} (cm^3g^{-1})	Wp (nm)
SBA-15	1040	1.38	7.1
CMK-3	1323	1.01	4.5
VxOy -CMK-3	1054	0.85	3.9
VxOy -SBA-15	678	0.75	6.5

V_{TP}: Total Volume Pore; S_{BET}: BET superficial area: WP: Pore diameter.

UV–Vis–DRS

Figure 4 shows the UV-Vis-DRS spectra of samples V_xO_y-CMK-3 and V_xO_y-SBA-15. Both samples with a Vanadium content determined by ICP and EDS of 1.3 wt.% and 2.5 wt.%, in CMK-3 and SBA-15 respectively, have a band at 260-270 nm and another around 340-500 nm. The first of these at a shorter wavelength indicates electronic transitions from O2- to V^{5+} that could be assigned to tetrahedral V^{5+} species of V_2O_5 [25, 26]; The second wavelength and very low proportion especially in CMK-3 would be due to "bulk-like" V_2O_5 crystallites due to the further polymerization of the V species [27-29].

A band approximately 450 nm is not detected, being attributed to bulk V_2O_5, which confirms that vanadium would be very highly isolated V_2O_5 species of small microcrystalline size, as indicated by the XRD and TEM studies.

X-Ray Photoelectron Spectroscopy

In the preliminary studies, the oxidation state of vanadium from V-MCM-41 sample was found as +5 from XPS peak of V (2p3/2) at 517.2 eV. A

distorted form of rutile is typical of monoclinic crystal structure of V_2O_4. V^{3+} ions are sixfold-coordinated by oxygen ions at two distinct distances is present in a corundum structure in which V is as V_2O_3. In some case according XANES V K-edge spectra in MCM-41, shows fivefolded V^{5+} as V_2O_5 [30].

Figure 5 shows the binding energy of V2p3/2 and V2p1/2 core level in V_xO_y-CMK-3 and SBA-15 samples. The only band observed at 517.3-517.2 eV for all samples is due to V_2O_5 with V^{5+}. The contribution due to V4+ centered at 516.3eV [31] is not observed. In this way, the V_2O_5 spectrum presents for the O1s core level spectrum a signal located around 531 and 532 eV, typical for V_2O_5 [32] presents. The shoulder which was not observed at 532.7-533 eV is attributed to oxygen associated with water chemisorbed (expressed as O 'α) [31].

The indication that most the V particles are in the porous and channels is the comparison between the XPS data (at 50–100 Å of deep) and EDS data (bulk information). Whereas by XPS the V/C= 0.00028 and V/Si =0.0024 (0.14 and 0.42 wt% respectively), by EDS nominal V was 1.28 and 2.5 wt.% for V_xO_y-CMK-3 and V_xO_y-SBA-15

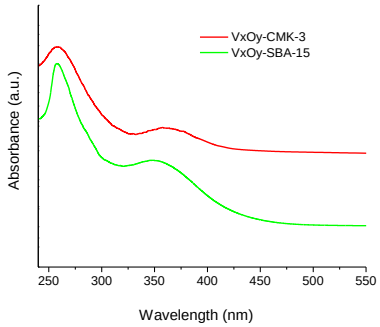

Figure 4. UV–Vis–DRS spectra of Vanadium containing-CMK-3 and SBA-15 samples.

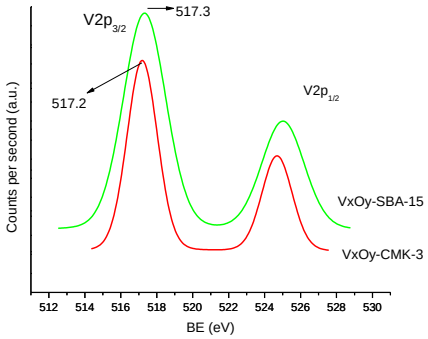

Figure 5. XPS of V containing SBA-15 and CMK-3 samples

Transmission Electron Microscopy

To obtain more information about the structure and size of the pores, TEM studies were performed (Figure 6). The TEM images of the samples in the direction [110], V_xO_y-SBA-15 (2.5% by weight V) and V_xO_y-CMK-3 (1.3% by weight V), indicate clearly visible to the pore arrangements ordered from the samples in the direction [110]. The pore sizes were in the range of 6-7nm for V containing-SBA-15 and 3.5-4.5nm for CMK-3[33], in agreement with the average pore sizes calculated by Isotherm BJH model of N_2 adsorption (Table 1). The TEM images of the grouped vanadium nanooxides are probably not seen due to a low contrast of the TEM- image.

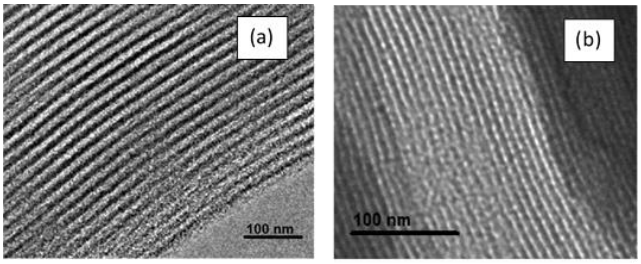

Figure 6. TEM images of (a) VxOy-SBA-15 and VxOy-CMK-3

Hydrogen uptakes measurements

As can be seen in figure 7 fit was used least-squares nonlinear regression for arbitrary fit functions and minimizing the objective function, employing Levenberg-Marquardt method. The experimental data was fitted by Freundlich isotherm equation that is an empirical formula for gaseous adsorbates. The Freundlich model is described previously. The fitting accuracy was R2=0.98. The capacity of hydrogen storage was evaluated at cryogenic temperatures (77 K). [15].

Figure 7 shows the adsorption–desorption isotherms of hydrogen at 77 K on CMK-3, SBA-15, V_xO_y-SBA-15 and V_xO_y-CMK-3 samples at a range of pressures (0-10 bar). The inset of this figure shows the behavior at low pressures (0-1 bar).

At low and high pressures, the amount of hydrogen uptake is higher in vanadium containing samples (V_xO_y-CMK-3 and V_xO_y-SBA-15) respect to its supports (CMK-3 and SBA-15). The process is fully reversible, the curve becomes in same place, since every point returns to initial values.

The hydrogen sorption onto SBA-15 was negligible but when vanadium is added the hydrogen uptake increases. The same behavior happens with carbon materials but the amount H_2 adsorption molecules is more important than siliceous materials.

The V_2O_5 nanoclusters increase the capacity of hydrogen adsorption in pristine materials. The

importance lies in the V^{5+} metal cation that is the main component that increase the capacity of this materials.

In general, "strong" chemical bonds are well studied but the study of the chemistry of the very-weak interactions is less known. There are two important charge transfer mechanisms in hydrogen sorption. In one hand, H_2 work as a weak Lewis base where charge is accepted from the adsorbent to the σ* orbital of hydrogen molecule. This interaction can be as weak, but can also be much stronger. In other hand, H_2 is a weak Lewis acid that donates charge from its σ orbital.

A significant contribution to the physisorption of H_2 can also have the polarization phenomena, producing electrostatic moments on H_2, and allowing an attractive electrostatic interaction with the linker. A strong local dipole or quadrupole moment can due to an H_2 polarizing environment.

When considering the interactions of H_2 with the V_xO_y-CMK-3 or V_xO_y-SBA-15 materials, could have three physisorption mechanisms: Non-metallated linkers, Fully-coordinated metallated bonds, Metallated linkers with strong electrostatic moments [34].

Where no metals exist (like CMK-3 or SBA-15) and there are no acceptor or donor groups on the linker, could occur weak charge transfer and dispersion forces are the only attractive events. Also in CMK-3 carbon the molecules of hydrogen spillover onto the CMK-3 nano/micropores like in activated carbons [16].

In Fully-coordinated metallated bonds, where closed shell coordinated metal ions are present, H_2 donates charge into fuzzy orbitals of Rydberg states on the metal in addition to the forces mentioned above. The charge transfer amount depends on the availability of the metal ion to the H_2 molecule.

For last case, (metallated linkers with strong electrostatic moments), can exists strong electrostatic moments that are compatible with H2, the attraction mechanism is mainly electrostatic, where electrostatic forces polarize and attract the H_2 molecule to the linker.

Supposing that weakly orbital interactions occur between the H_2 and the metal nanocluster, therefore physisorption is the main interaction, all cases has the potential to uptake H_2 weakly as physorption process and the last interaction achieves sufficiently strong energies to storage more hydrogen to reach the level adsorption in V_xO_y-CMK-3. In addition, no hydrogen chemisorption was detected.

The first layer of hydrogen molecules may be reacted with the metal cation in oxide cluster linking like as dihydrogen complex (Kubas interaction) [35]. More hydrogen molecules are adsorbed by dipole-induced interaction in a second layer due to that strong interaction of the metal particles takes dipole inducing forces in hydrogen molecules. Upper layers could interact with metallic cation by dipole-induce bond but interaction force decrease when the distance to the surface increases. CMK-3 carbon helps to better disperse the V_2O_5 clusters (V_xO_y-CMK-3 sample), therefore, clusters are smaller and higher active surface for the adsorption of H_2 is created than in V_xO_y-SBA-15.

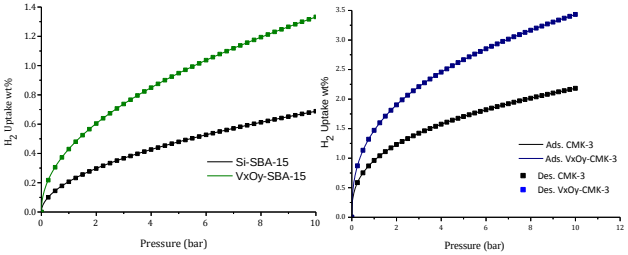

Figure 7. Hydrogen adsorption–desorption isotherms of CMK-3, SBA-15 and V containing-CMK-3 and SBA-15

4. Conclutions

An important conclusion of this work concerns the design of vanadium oxide (V_2O_5)-decorated ordered mesoporous carbon CMK-3 and mesoporous silica SBA-15.

The materials synthesized are promising in hydrogen uptake by weak links forces (physisorption). The activity of samples is ascribed to the improved dispersion of uniform vanadium nanoparticles as well as to properly use of the support, which may probably originate a high surface area and pore volume, allowing a large dispersion of vanadium.

V^{5+} cation in V_2O_5 is an active specie to uptake and storage hydrogen by a physisorption process and the support plays an important role in metal cluster dispersion and size.

Moreover, V_2O_5 nanoclusters are within the nanopores of CMK-3, according to XPS and EDS analysis, this confirms the high dispersion of these clusters because the largest area of the supports are existing in the walls of their inner channels.

The mesoporous carbon adsorbs more hydrogen than the SBA-15 material due to a high spillover of hydrogen molecules in the framework that also contributes to a greater diffusion of the hydrogen to the metallic clusters surface.

A hydrogen storage mechanism on V_2O_5 cluster surfaces was proposed. The procedure of this adsorption is still under further research and

optimization.

Assuming that no strong orbital interactions occur between the H_2 and the V^{5+} cation, such that physisorption is the main interaction, the first layer interact by Kubas interaction that to have the potential to achieve sufficiently strong interaction energies to reach the desired target range.

Hydrogen storage behaviors onto V_2O_5–CMK-3 can be optimized by controlling metal cluster size, dispersion and the nature of support by increasing framework-specific surface area. The preparation of metal sites on the proper support, leaving the metal mostly exposed is expected to be a main experimental challenge, as these metal sites are expected to interact with more hydrogen molecules.

5. Referencias

[1] G.W. Crabtree, M.S. Dresselhaus, MRS Bull. 33 (2008) 421.

[2] P. Dibandjo, C. Zlotea, R. Gadiou, C.M. Ghimbeu, F. Cuevas, M. Latroche M, et al. Int J Hydrogen Energy, 38 (2013) 952.

[3]Office of Energy Efficiency & Renewable Energy: https://energy.gov/eere/ fuelcells/hydrogen-storage.

[4] M. Bastos-Neto, C. Patzschke, M. Lange, J. Mollmer, A. Moller, S. Fichtner, C. Schrage, D. Lassig, J. Lincke, R. Staudt, H. Krautscheid, R. Glaser, Energy Environ. Sci. 5 (2012) 8294.

[5] S. Satyapal, J. Petrovic, C. Read, G. Thomas, G. Ordaz, Catal. Today 120 (2007) 246.

[6]T-H. Fang, W-J. Chang, C-C. Huang, W-L. Sun, Int J Hydrogen Energy, 41 (2016) 13771.

[7]S. Schaefer, V. Fierro, M.T. Izquierdo, A. Celzard, Int J Hydrogen Energy, 41 (2016) 12146.

[8] W. Zhao, V. Fierro, C. Zlotea, E. Aylon, M.T. Izquierdo, M. Latroche M et al, Int J Hydrogen Energy, 36 (2011) 11746.

[9] H. Zang, D. Zhao, J. Mater. Chem. 15 (2005) 1217.

[10] M. Anbia, A. Ghaffari, Appl. Surf. Sci. 255 (2009) 9487.

[11] M. Anbia, Z. Parvin, Chem. Eng. Res. Des. 89 (2011) 641.

[12]R. Schmidt, M. Stöcker, E.W. Hansen, et al. Microporous Mater. 3 (1995) 443.

[13] G. Soler-Illia, C. Sanchez, B. Lebeau, et al. Chem. Rev. 102 (2002) 4093.

[14] J. M. Juárez, M. B. Gómez Costa, O. A. Anunziata, Int. J. Energy Res. 39 (2015) 128.

[15] J. M. Juárez, M. B. Gómez Costa, O. A. Anunziata, Int. J. Energy Res. 39 (2015) 941.

[16] M. B. Gómez Costa, J. M. Juárez, G. Pecchi and O. A. Anunziata. Bulletin of Materials Science 40 (2017) 271.

[17]M. Konni, A.S. Dadhich, S.B. Mukkamala, Int J Hydrogen Energy 42 (2017) 953.

[18] V. Meynen, P. Cool, E.F. Vansant, Microporous and Mesoporous Materials, 125 (2009)170.

[19] H.Yang, D. Zhao D, Journal of Material Chemistry, 15 (2005) 1217.

[20] H. Huwe, M. Fröba, Microporous and Mesoporous Materials, 60 (2003) 151.

[21]D. Zhao, J. Feng, Q. Huo, N. Melosh, G. Fredrickson, B. Chmelka, G. Stucky, Science, 279 (1998) 548.

[22] U. Suryavanshi, T. Iijima, A. Hayashia, Y. Hayashi, M. Tanemura, Chemical Engeneering Journal, 179 (2012) 388.

[23]J. Goscianska, A. Olejnik, I. Nowak, M. Marciniak, R. Pietrzak, European Journal of Pharmaceutics and Biopharmaceutics, 94 (2015) 550.

[24] M. B. Gómez Costa, J. M. Juárez, M.L. Martínez, A.R. Beltramone, J. Cussa, O.A. Anunziata, Material Reseach Bulletin, 48 (2013) 661.

[25] M.A. Larrubia, G. Busca, Mater. Chem. Phys. 72 (2001) 337.

[26] P. Concepción, M.T. Navarro, T. Blasco, J.M. López Nieto, B. Panzacchi, F. Rey, Catal. Today. 96 (2004) 179.

[27] K. Chen, E. Iglesia, A.T. Bell, J. Catal. 192 (2000) 197.

[28] M. Baltes, K. Cassiers, P. Van der Voort, B.M. Weckhuysen, R.A. Schoonheydt, E.F. Vansant, J. Catal. 197 (2001) 160.

[29] J.L. Male, H.G. Niessen, A.T. Bell, T.D. Tilley, J. Catal. 194 (2000) 431.

[30] O. A. Anunziata, A. R. Beltramone, J. Cussa, Catalysis Today, 133 (2008) 891.

[31] J. Fang, X. Bi, D. Si, Z. Jiang, W. Huang, Appl. Surf. Sci. 253 (2007) 8952

[32] M.D. Soriano, J.A. Cecilia, A. Natoli, J. Jiménez, J.M. López Nieto,E. Rodríguez-Castellón, Catal. Today. 254 (2015) 36.

[34] Fei Gao,Yanhua Zhang, HaiqinWan, YanKong, Xingcai Wu, ,LinDong, Baiqin Li, Yi Chen. Microporous and Mesoporous Materials. 110 (2008) 508.

[35] E. Tsivion, R. Jeffrey, R. Long, M. Head-Gordon, J. Am. Chem. Soc., 136 (2014) 17827.

[36] Y. Takasu, R. Unwin, B. Tesche, A.M. Bradshaw, M. Grunze, Surf. Sci. 77 (1978) 219.